

Ion Transfer at the Interface between Water and a Fluorous Solvent 1,1,1,2,3,4,4,5,5,5-Decafluoropentane

Kohei UEMATSU^{1,*}, Hajime KATANO¹, Yasuhiro KURODA¹ and Toshiyuki OSAKAI²

¹*Department of Bioscience, Fukui Prefectural University, Eiheiji, Fukui 910-1195, Japan;*

²*Department of Chemistry, Kobe University, Nada, Kobe 657-8501, Japan*

Ion-transfer reactions at the interface between fluoruous solvent 1,1,1,2,3,4,4,5,5,5-decafluoropentane (DFP) and water (W) were investigated voltammetrically. Within the potential window at the DFP | W interface, various non-fluorinated ions, including tetraphenylarsonium (Ph_4As^+) and tetraphenylborate (Ph_4B^-), and fluorinated ions gave reversible voltammetric waves for their ion transfer across the DFP | W interface. Based on the Ph_4As^+ - Ph_4B^- assumption, the formal potentials of their ion transfer could be determined in terms of Galvani potential difference. The formal Gibbs energies for the transfer of ions from DFP to W, which would provide the criteria necessary for evaluating the fluorophilicity/hydrophilicity of ions were calculated from the formal potentials, and were compared with the transfer energies from 1,2-dichloroethane to W and those from DFP to the organic solvent, as quantitative scales of the ion's lipophilicity/hydrophilicity and fluorophilicity/lipophilicity.

1. Introduction

Electrochemical processes at a liquid | liquid or non-aqueous solvent | W interface have been studied extensively, because of the wide range of applicability of the systems in chemistry and biology. It is necessary for the non-aqueous solvent that it is immiscible with W and forms stable interface, and that it dissolves high concentration of electrolyte to give a high conductivity. To date, nitrobenzene (NB), 1,2-dichloroethane (DCE), and their analogues have been used as non-aqueous solvents in liquid-liquid electrochemistry. In a previous paper [1], we examined the applicability of a fluoruous solvent DFP as a non-aqueous phase for ion-transfer voltammetry. In this study, we have investigated the transfer of various monovalent ions across the DFP | W interface. Interestingly, unlike the DCE | W and NB | W interfaces, Ph_4As^+ and Ph_4B^- ions gave voltammetric waves within the potential window of the DFP | W interface. The voltammograms could be attributed to the reversible transfer of monovalent ions, and the reversible half-wave potentials, ${}^rE_{1/2}(\text{Ph}_4\text{As}^+)$ and ${}^rE_{1/2}(\text{Ph}_4\text{B}^-)$, were determined. On the basis of the Ph_4As^+ - Ph_4B^- extrathermodynamic assumption, the formal potentials for the transfer of these ions in terms of the Galvani potential difference at the DFP | W interface, $\Delta_{\text{DFP}}^{\text{W}}\phi^{0^0}(\text{Ph}_4\text{As}^+)$ and $\Delta_{\text{DFP}}^{\text{W}}\phi^{0^0}(\text{Ph}_4\text{B}^-)$, were calculated from the ${}^rE_{1/2}$ values. Other ions (j^z , z being the charge number including sign) also gave reversible voltammetric waves, and their $\Delta_{\text{DFP}}^{\text{W}}\phi^{0^0}(j^z)$ values were determined. From the $\Delta_{\alpha}^{\text{W}}\phi^{0^0}(j^z)$ values ($\alpha = \text{DFP}$, DCE , and NB), the formal Gibbs transfer energy of j^z ion from the α to the W phase, $\Delta G_{\text{tr},\alpha \rightarrow \text{W}}^{0^0}(j^z)$, were calculated by

$$\Delta G_{tr,\alpha \rightarrow W}^{0,}(j^z) = -zF\Delta_{\alpha}^W\phi^{0,}(j^z). \quad (1)$$

Although DFP is miscible with DCE (and NB), the transfer energy of j^z ion from DCE to DFP is calculated by

$$\Delta G_{tr,DCE \rightarrow DFP}^{0,}(j^z) = \Delta G_{tr,DCE \rightarrow W}^{0,} - \Delta G_{tr,DFP \rightarrow W}^{0,}. \quad (2)$$

The $\Delta G_{tr,DFP \rightarrow W}^{0,}$, $\Delta G_{tr,DCE \rightarrow W}^{0,}$, and $\Delta G_{tr,DCE \rightarrow DFP}^{0,}$ values can be useful as quantitative scales of the affinities for the fluorous solvent, water, and the non-fluorinated organic solvent, that is, fluorophilicity, hydrophilicity and lipophilicity of ions. These values of non-fluorinated and fluorinated ions were compared with each other.

2. Experimental

2.1 Reagents

The purification of DFP and the preparation of supporting electrolytes for the DFP phase, tetra-*n*-octylammonium bis(nonafluorobutanesulfonyl)imide (Oct₄NBNSI) and tetrabutylammonium tetrakis[3,5-bis(trifluoromethyl)phenyl]borate (Bu₄NTPPB) were described in Ref. 1. Ph₄AsBNSI and Bu₄N⁺ salts with [(C_nF_{2n+1}SO₂)₂N]⁻ at *n* = 1, 2, and 3 (BTSI⁻, BPSI⁻ and BHSI⁻) were prepared in a manner similar to that used to prepare Oct₄NBNSI or Bu₄NBNSI. Other chemicals were of reagent grade and used as received.

2.2 Measurements

Ion-transfer reactions across the DFP | W interface have been studied by means of cyclic voltammetry using a three-electrode system. Cells I and II represent the electrochemical cells used to record the cyclic voltammograms (CVs) of the transfer of the Ph₄As⁺ and Ph₄B⁻ ions across the DFP | W interface, respectively.

cell I:

	Phase I	Phase II *	Phase III	Phase IV	
Pt	<i>a</i> mM Ph ₄ AsBNSI 0.1 M Oct ₄ NBNSI	<i>a</i> mM Ph ₄ AsBNSI 0.1 M Oct ₄ NBNSI	0.05 M MgSO ₄	0.1 M LiCl	AgCl Ag
(CE)	(DFP)	(DFP)	(W)	(W)	(RE1)
AgCl Ag	Phase V 0.1 M LiCl 0.1 M 0.1 M LiOH HBNSI	Phase VI 0.1 M Oct ₄ NBNSI			
(RE2)	(W)	(DFP)			

cell II:

	Phase I	Phase II *	Phase III	Phase IV	
Pt	0.1 M Bu ₄ NBNSI	0.1 M Bu ₄ NTPPB	<i>b</i> mM NaPh ₄ B 0.1 M LiCl	0.1 M LiCl	AgCl Ag
(CE)	(DFP)	(DFP)	(W)	(W)	(RE1)
AgCl Ag	Phase V 0.1 M Bu ₄ NCl	Phase VI 0.1 M Bu ₄ NTPPB			
(RE2)	(W)	(DFP)			

The test DFP | W interface is indicated by an asterisk. The electrolysis cell is described in Ref. 1. The solution resistance between the two reference electrodes was about 2 kΩ for cells I and II. *E* was controlled by a potentiostat furnished with a positive feedback *iR* compensation circuit. In this paper, the *E* value is reported against the ${}_rE_{1/2}$ for transfer of the tetramethylammonium (Me₄N⁺) ion across the DFP | W interface, which was determined to be ${}_rE_{1/2}(\text{Me}_4\text{N}^+) = -0.276$ V with cell I and 0.334 V with cell II. All electrochemical measurements were carried out at 25±1°C.

3. Results and Discussion

3.1 Physical properties of DFP

At 25°C, the solubility of W in DFP is 0.049 wt% [1], and the density of DFP is 1.58 g cm⁻³. Therefore, DFP formed a stable interface with W. The relative permittivity of DFP is 6.72, which is lower than those of DCE (10.45) and NB (34.78). Despite the low permittivity, DFP dissolves an electrolyte Oct₄NBNSI at the 0.1 M level, and the conductivity of the 0.1 M Oct₄NBNSI (DFP) was 220 μS/cm, which is comparable to those of the DCE and NB solutions (910 and 690 μS/cm). The viscosity of DFP was determined to be 0.90 cP by a vibro viscometer. The value is very close to that of W. On the basis of Walden rule, the ratio of the diffusion coefficient of a *j*^z ion in the W phase to that in the DFP phase, D_j^W/D_j^{DFP} , is assumed to be $D_j^W/D_j^{DFP} \approx 1$ in the determination of $\Delta_{DFP}^W \phi^{0z}(j^z)$ below.

3.2 Transfer of Ph₄As⁺ and Ph₄B⁻ ions at the DFP | W interface

Curve (a) in Figure 1 shows a CV obtained with cell I at $a = 0$, that is, the base current of the 0.1 M Oct₄NBNSI (DFP) | 0.05 M MgSO₄ (W) interface at the scan rate of $\nu = 0.1$ V s⁻¹. A polarizable potential window was observed. Curve (b) in the figure shows a CV obtained with cell I at $a = 0.5$ and $\nu = 0.1$ V s⁻¹. Within the potential window, a pair of well-defined cathodic and anodic peak currents were observed, corresponding to the transfer of the Ph₄As⁺ ion from the DFP to the W phase and back to the DFP phase, respectively. The dependence of the height of anodic peak current and the potential peak

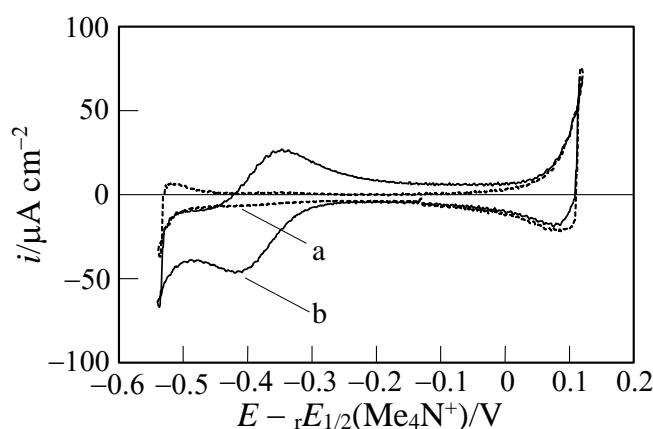


Figure 1. Cyclic voltammograms (CVs) at the 0.1 M Oct₄NBNSI (DFP) | 0.05 M MgSO₄ (W) interface in the (a) absence and (b) presence of 0.5 mM Ph₄AsBNSI in the DFP phase. Scan rate, $\nu = 0.1$ V s⁻¹.

separation on ν indicates that the voltammogram can be assigned to a reversible CV of monovalent ion transfer. By taking that the reversible half-wave potential is equal to the midpoint potential, the $rE_{1/2}(\text{Ph}_4\text{As}^+)$ was determined to be -0.387 ± 0.004 V vs. $rE_{1/2}(\text{Me}_4\text{N}^+)$.

Curve (a) in Figure 2 shows a CV obtained with cell II at $b = 0$. By the replacement of the electrolyte anion, the anodic final rise was shifted to a more positive potential range. Curve (b) in the figure shows a CV obtained with cell II at $b = 0.1$. The anodic and cathodic voltammetric waves can be attributed to the transfer of the Ph₄B⁻ ion from the W to the DFP phase and back to the W phase, respectively. The voltammogram can be assigned to a reversible CV of monovalent ion transfer, and the reversible half-wave potential $rE_{1/2}(\text{Ph}_4\text{B}^-)$ was determined to be 0.067 ± 0.005 V vs. $rE_{1/2}(\text{Me}_4\text{N}^+)$.

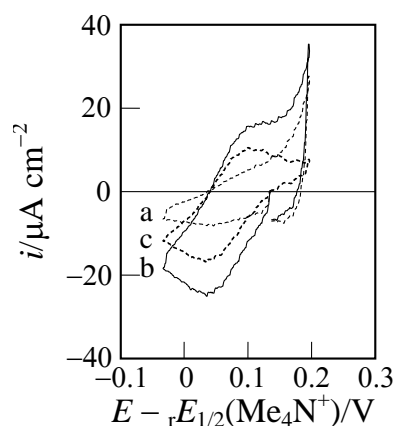


Figure 2. CVs at the 0.1 M Bu₄NTFPB (DFP) | 0.1 M LiCl (W) interface in the (a) absence and (b) presence of 0.1 mM NaPh₄B in the W phase. $\nu = 0.1$ V s⁻¹. (c), (b) - (a).

The reversible half-wave potential of a j^z ion, ${}_{r}E_{1/2}(j^z)$, can be related to $\Delta_{DFP}^W\phi^{0^z}(j^z)$, as given by

$${}_{r}E_{1/2}(j^z) = \Delta_{DFP}^W\phi^{0^z}(j^z) + (RT/zF)\ln[(D_j^W/D_j^{DFP})^{1/2}] + \Delta E_{ref} \quad (3)$$

where ΔE_{ref} is determined by the reference electrode system for cells I and II. R , T , and F are used in the usual meaning. By taking $D_j^W/D_j^{DFP} = 1$, that is, $(RT/zF)\ln[(D_j^W/D_j^{DFP})^{1/2}] = 0$, and $\Delta_{DFP}^W\phi^{0^z}(\text{Ph}_4\text{As}^+) + \Delta_{DFP}^W\phi^{0^z}(\text{Ph}_4\text{B}^-) = 0$, the formal potentials are calculated to be $\Delta_{DFP}^W\phi^{0^z}(\text{Ph}_4\text{As}^+) = -0.227 \pm 0.006$ V, $\Delta_{DFP}^W\phi^{0^z}(\text{Ph}_4\text{B}^-) = 0.227 \pm 0.006$ V, and $\Delta_{DFP}^W\phi^{0^z}(\text{Me}_4\text{N}^+) = 0.160 \pm 0.006$ V. Also, ΔE_{ref} values were calculated to be -0.365 and 0.174 V for cells I and II, respectively.

3.3 Formal potentials for the transfer of ions at DFP | W interface

The CVs of the transfer of choline (Ch^+), acetylcholin (ACh^+), tetraethylammonium (Et_4N^+), tetrapropylammonium (Pr_4N^+), and Bu_4N^+ cations and 2,4,6-trinitrophenolate (TNP^-), 2,4-dinitrophenolate (DNP^-), ClO_4^- , SCN^- , Γ^- , NO_3^- , and Br^- anions at the DFP | W interface were recorded with cell I, in which Phase III (W) was replaced by 0.50 mM $j^+\text{Cl}^-$ ($j^+ = \text{Ch}^+$, and ACh^+), $j^+\text{Br}^-$ ($j^+ = \text{Et}_4\text{N}^+$, Pr_4N^+ , and Bu_4N^+), or Na^+J^- ($\text{J}^- = \text{TNP}^-$, DNP^- , ClO_4^- , SCN^- , Γ^- , NO_3^- , and Br^-) and 0.05 M MgSO_4 (W), and Phases I and II were replaced by 0.1 M Oct_4NBNSI (DFP). These ions gave well-developed voltammetric waves within the potential window, and the voltammetric behaviors were of reversible nature. Using $\Delta E_{ref} = -0.365$ V, the $\Delta_{DFP}^W\phi^{0^z}(j^z)$ values were determined as listed in Table 1 together with the reported values of $\Delta_{DCE}^W\phi^{0^z}$ [2] and $\Delta_{NB}^W\phi^{0^z}$ [3-5].

Fluorocomplex anions, BF_4^- and PF_6^- , perfluoro- n -alkanoate anions, $\text{C}_n\text{F}_{2n+1}\text{COO}^-$ with $n = 1, 2, 3$, and 4 (TFA^- , PFP^- , HFB^- , and NFP^- , respectively), and BTSI^- anion gave reversible CVs within the potential window at the 0.1 M Oct_4BNSI (DFP) | 0.05 M MgSO_4 (W) interface, and their formal potentials were determined as listed in Table 2. The formal potential for the transfer of the BPSI^- , and BHSI^- were determined by the EMF measurement as listed in the table.

3.4 Formal Gibbs transfer energy

The possible ion-pair formation of tested ions with electrolyte ions in DFP is currently studied, so at present we cannot make a meticulous discussion of the standard potentials for the transfer of ions at the DFP | W interface. However, the determined formal potentials, though

Table 1. Formal potentials for the transfer of non-fluorinated ions at the DFP, DCE, and NB | W interfaces, $\Delta_{DFP}^W\phi^{0^z}$, $\Delta_{DCE}^W\phi^{0^z}$, and $\Delta_{NB}^W\phi^{0^z}$ (in V)

ion	$\Delta_{DFP}^W\phi^{0^z}$	$\Delta_{DCE}^W\phi^{0^z}$ a)	$\Delta_{NB}^W\phi^{0^z}$ b)
cation			
Ch^+	0.223±0.004	0.200	0.117
Me_4N^+	0.160±0.006	0.133	0.035
ACh^+	0.140±0.002	0.110	0.049
Et_4N^+	0.036±0.003	-0.013	-0.055
Pr_4N^+	-0.087±0.003	-0.141	-0.170
Bu_4N^+	-0.189±0.005	-0.278	-0.275
Ph_4As^+	-0.227±0.006	-0.341	-0.372
anion			
Ph_4B^-	0.227±0.006	0.345	0.372
TNP^-	-0.016±0.003	0.043	0.069
ClO_4^-	-0.097±0.003	-0.078	-0.082
DNP^-	-0.113±0.004	-0.083	-0.076
SCN^-	-0.197±0.003	-0.161	-0.164
Γ^-	-0.227±0.004	-0.179	-0.191
NO_3^-	-0.241±0.003	-0.258	-0.261
Br^-	-0.318±0.004	-0.289	-0.288

a) Ref. 2, b) Refs. 3-5.

Table 2. $\Delta_{DFP}^W\phi^{0^z}$ and $\Delta_{DCE}^W\phi^{0^z}$ for fluorinated ions (in V).

ion	$\Delta_{DFP}^W\phi^{0^z}$	$\Delta_{DCE}^W\phi^{0^z}$
BHSI^-	0.317±0.001	0.206±0.004
BPSI^-	0.217±0.002	0.142±0.004
BTSI^-	0.132±0.002	0.078±0.004
PF_6^-	0.063±0.004	0.041±0.004
NFP^-	-0.099±0.002	-0.103±0.002
BF_4^-	-0.113±0.003	-0.097±0.003
HFB^-	-0.156±0.002	-0.140±0.002
PFP^-	-0.199±0.002	-0.181±0.002
TFA^-	-0.264±0.003	— ^{a)}

a) Out of the potential window.

involving the contribution of ion-pair formation, may be useful to discuss the hydrophilic, hydrophobic, or fluorophilic nature of the ions. From the values of $\Delta_{\text{DFP}}^{\text{W}}\phi^{0,}$ and $\Delta_{\text{DCE}}^{\text{W}}\phi^{0,}$, $\Delta G_{\text{tr,DFP}\rightarrow\text{W}}^{0,}$, $\Delta G_{\text{tr,DCE}\rightarrow\text{W}}^{0,}$, and $\Delta G_{\text{tr,DCE}\rightarrow\text{DFP}}^{0,}$ were calculated by Eqs. (1) and (2), as listed in Table 3.

In Fig. 3, $\Delta G_{\text{tr,DFP}\rightarrow\text{W}}^{0,}$ for non-fluorinated ions is plotted against $\Delta G_{\text{tr,DCE}\rightarrow\text{W}}^{0,}$ as shown by the filled circles. The plot gives the regression line:

$$\Delta G_{\text{tr,DFP}\rightarrow\text{W}}^{0,} / \text{kJ mol}^{-1} = (0.84 \pm 0.040)(\Delta G_{\text{tr,DCE}\rightarrow\text{W}}^{0,} / \text{kJ mol}^{-1}) + (-4.9 \pm 0.9), \quad (4)$$

with the correlation coefficient of 0.993. Despite the differences in the sign of the charge and in the structure among the ions tested, an excellent linear relationship was observed between $\Delta G_{\text{tr,DFP}\rightarrow\text{W}}^{0,}$ and $\Delta G_{\text{tr,DCE}\rightarrow\text{W}}^{0,}$. Such an excellent linear relationship was also observed between $\Delta G_{\text{tr,DFP}\rightarrow\text{W}}^{0,}$ and $\Delta G_{\text{tr,NB}\rightarrow\text{W}}^{0,}$.

Despite the richness of fluorine atoms, TFA^- , PF_6^- , HFB^- , BF_4^- , and NFP^- ions gave negative $\Delta G_{\text{tr,DFP}\rightarrow\text{W}}^{0,}$ values. Since their $\Delta G_{\text{tr,DCE}\rightarrow\text{W}}^{0,}$ values were also negative, and these ions can be categorized as hydrophilic. This category of ions is not bulky, so their surfaces have higher electric field strength. Therefore, the electrostatic (*i.e.*, coulomb and polarization) ion-solvent interactions would contribute significantly to the Gibbs transfer energy. On the other hand, the PF_6^- , BTSI^- , BPSI^- , and BHSI^- ions gave positive $\Delta G_{\text{tr,DCE}\rightarrow\text{W}}^{0,}$ values, and thus can be categorized as hydrophobic. The $\Delta G_{\text{tr,DFP}\rightarrow\text{W}}^{0,}$ for fluorinated ions is plotted against $\Delta G_{\text{tr,DCE}\rightarrow\text{W}}^{0,}$ as shown by the open circles in Fig. 3. The $\Delta G_{\text{tr,DFP}\rightarrow\text{W}}^{0,}$ values for the hydrophilic fluorinated ions are close to their $\Delta G_{\text{tr,DCE}\rightarrow\text{W}}^{0,}$. However, the $\Delta G_{\text{tr,DFP}\rightarrow\text{W}}^{0,}$ values for the hydrophobic fluorinated ions are higher than those predicted from Eq. (4) with increasing $\Delta G_{\text{tr,DCE}\rightarrow\text{W}}^{0,}$, that is, the hydrophobicity of the ions.

As another representation, the values of $\Delta G_{\text{tr,DCE}\rightarrow\text{DFP}}^{0,}$ are plotted against those of $\Delta G_{\text{tr,DCE}\rightarrow\text{W}}^{0,}$ in Fig. 4. $\Delta G_{\text{tr,DCE}\rightarrow\text{DFP}}^{0,}$ could be used as a quantitative scale of fluorophilicity/lipophilicity of ions. The plots of $\Delta G_{\text{tr,DCE}\rightarrow\text{DFP}}^{0,}$ for hydrophilic ions are concentrated in the vicinity of the abscissa axis, *i.e.*, at $\Delta G_{\text{tr,DCE}\rightarrow\text{DFP}}^{0,} = 0$. The $\Delta G_{\text{tr,DCE}\rightarrow\text{DFP}}^{0,}$ for hydrophobic fluorinated ions, however, shifted to more negative values with increasing $\Delta G_{\text{tr,DCE}\rightarrow\text{W}}^{0,}$, *i.e.*, the hydrophobicity of the ions. On the other hand, $\Delta G_{\text{tr,DCE}\rightarrow\text{DFP}}^{0,}$ for hydrophobic non-fluorinated ions shifted to more positive values with increasing $\Delta G_{\text{tr,DCE}\rightarrow\text{W}}^{0,}$. These results suggest that fluorophilicity of ions should be a physical property incompatible with both lipophilicity and hydrophilicity.

Table 3. Formal Gibbs transfer energy of tested ions from DFP to W, $\Delta G_{\text{tr,DFP}\rightarrow\text{W}}^{0,}$, from DCE to W, $\Delta G_{\text{tr,DCE}\rightarrow\text{W}}^{0,}$, and from DCE to DFP, $\Delta G_{\text{tr,DCE}\rightarrow\text{DFP}}^{0,}$ (in kJ mol^{-1}).

ion	$\Delta G_{\text{tr,DFP}\rightarrow\text{W}}^{0,}$	$\Delta G_{\text{tr,DCE}\rightarrow\text{W}}^{0,}$	$\Delta G_{\text{tr,DCE}\rightarrow\text{DFP}}^{0,}$
cation			
Ch^+	-21.5	-19.3	2.2
Me_4N^+	-15.4	-12.8	2.6
ACh^+	-13.5	-10.6	2.9
Et_4N^+	-3.5	1.3	4.7
Pr_4N^+	8.4	13.6	5.2
Bu_4N^+	18.2	26.8	8.6
Ph_4As^+	21.9	32.9	11.0
anion			
Ph_4B^-	21.9	33.3	11.4
TNP^-	-1.5	4.1	5.7
ClO_4^-	-9.4	-7.5	1.8
DNP^-	-10.9	-8.0	2.9
SCN^-	-19.0	-15.5	3.5
I^-	-21.9	-17.3	4.6
NO_3^-	-23.3	-24.9	-1.6
Br^-	-30.7	-27.9	2.8
fluorinated			
BHSI^-	30.6	19.9	-10.7
BPSI^-	20.9	13.7	-7.2
BTSI^-	12.9	7.5	-5.4
PF_6^-	6.1	4.0	-2.1
NFP^-	-9.6	-9.9	-0.4
BF_4^-	-10.9	-9.4	1.5
HFB^-	-15.1	-13.5	1.5
PFP^-	-19.2	-17.5	1.7

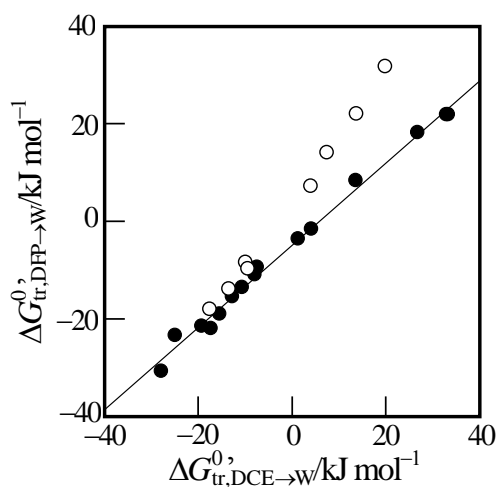


Figure 3. Plots of the formal Gibbs transfer energy from DFP to W, $\Delta G_{tr,DFP \rightarrow W}^0$, against that from DCE to W, $\Delta G_{tr,DCE \rightarrow W}^0$, for non-fluorinated (●) and fluorinated (○) ions.

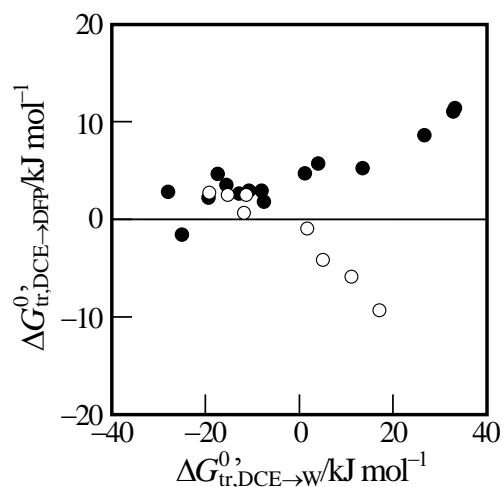


Figure 4. Plots of the formal Gibbs transfer energy from DCE to DFP, $\Delta G_{tr,DCE \rightarrow DFP}^0$, against $\Delta G_{tr,DCE \rightarrow W}^0$, for non-fluorinated (●) and fluorinated (○) ions.

4. Conclusions

The transfer of ions at the interface between a fluoruous solvent DFP and water could be studied voltammetrically, and the electrochemical data gave the formal Gibbs transfer energy of various ions from DFP to water or organic solvents, which can provide useful criteria for evaluating the fluorophilicity, lipophilicity, and hydrophilicity of ions. The transfer energy would be also useful to understand the interfacial process in solvent extraction using fluoruous solvents and compounds.

References

- 1) H. Katano, Y. Kuroda, K. Uematsu, *J. Electroanal. Chem.*, **788**, 232-234 (2017).
- 2) H. Katano, H. Tatsumi, M. Senda, *Talanta*, **63**, 185-193 (2004) 185.
- 3) T. Osakai, K. Ebina, *J. Phys. Chem. B*, **102**, 5691-5968 (1998).
- 4) J. Koryta, *Electrochim. Acta*, **29**, 445-452 (1984).
- 5) Z. Samec, D. Homolka, V. Mereček, L. Kavan, *J. Electroanal. Chem.*, **145**, 213-218 (1983).